

# Removing Imaging Artefacts in Wire Media Based Hyperlenses

Md. Samiul Habib<sup>1,\*</sup>, Shaghik Atakaramians<sup>1,2</sup>, Simon C. Fleming<sup>1</sup>, Alexander Argyros<sup>1</sup>, and Boris T. Kuhlmeiy<sup>1,2</sup>

<sup>1</sup>Institute of Photonics and Optical Science (IPOS), School of Physics, The University of Sydney, NSW 2006, Australia

<sup>2</sup>Centre for Ultrahigh Bandwidth Devices for Optical Systems (CUDOS), School of Physics, The University of Sydney, NSW 2006, Australia

\*samiul.habib@sydney.edu.au

**Abstract-** Imaging devices based on wire media (WM) can transmit deep subwavelength information over optically long distances by supporting high spatial frequencies. However, for perfect imaging WM need to be used at the Fabry-Perot resonances (FPRs), to avoid resonances of evanescent waves detrimental to image quality. Another source of artefacts are diffracting ordinary waves, which may add noise to the image. The role of ordinary waves becomes dominant when attempting to image large objects. Here we introduce novel approaches to removing artefacts in WM based hyperlenses so that they can be used for broadband imaging.

## I. INTRODUCTION

Recently, hyperbolic metamaterials have gained much attention in the research community due to their exciting properties [1], in particular for imaging: They possess extraordinary modes, which are propagating at high spatial frequencies and can be used to beat the diffraction limit [1-2]. A special kind of hyperbolic metamaterial is the wire medium (WM), composed of parallel, thin wires with subwavelength separation hosted within a dielectric [3]. WM based hyperlenses operate in the so called “canalization regime” [4], where evanescent waves are converted to propagating waves with constant phase velocity and low loss [3-5], making them promising candidates for subwavelength imaging. In 2010, our group fabricated WM by using the fibre drawing technique [6], and experimentally demonstrated magnifying and non-magnifying hyperlenses in the THz spectrum [7]. Recent theoretical and experimental reports on WM based hyperlenses have revealed that for perfect imaging, WM need to be tuned to the FPRs, where transmission amplitude and phase are independent of spatial frequency [2-3]. However, away from FPRs, images deteriorate due to resonant enhancement of evanescent waves at certain spatial frequencies resulting in image artefacts. These unwanted artefacts limit the use of hyperlenses for broadband subwavelength imaging. Furthermore, diffracting ordinary waves may add unwanted noise to the images when attempting to image large objects [8]. Here, we present post-processing methods to remove the imaging artefacts, so that imaging can be performed over wide frequency bands.

## II. RESULTS AND DISCUSSIONS

Figure 1 (a) shows a schematic of the studied WM, consisting of silver wires of 10  $\mu\text{m}$  diameter and 50  $\mu\text{m}$  pitch hosted in air. The length of the wires is  $L=1$  mm; an aperture (diameter

200  $\mu\text{m}$ , subwavelength for frequencies below 0.7 THz) is used as object to be imaged. We calculate images using CST microwave studio at fixed frequencies, exciting the aperture with an  $x$ -polarized plane wave propagating in the direction of the wires (along  $z$ ), and we image using the  $x$  component of the field,  $E_x$ . In Fig. 1(b) the field intensity is plotted as a function of position and frequency, which is referred as line-scan [7]. It is seen that the 200  $\mu\text{m}$  aperture is well resolved at all FPRs but strong periodic side lobes every  $\sim 150$  GHz appear away from the FPRs, and thus severely deteriorate imaging performance. The artefacts arise from reflections supported by WM which are constructively interfering [2, 9].

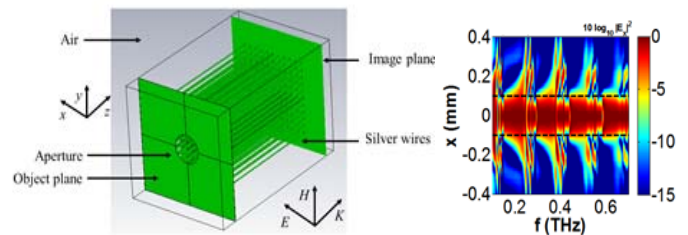


Fig. 1. (a) Schematic of the WM based hyperlens. (b) Simulated field intensity as a function of frequency and position at output of 1 mm long WM. The dotted lines indicate location of the aperture and output is taken 50  $\mu\text{m}$  away from the end of the WM.

These reflections can be eliminated by using a short electromagnetic pulse and time resolved measurements, which allow separating back reflections from the main pulse [9]. However such time resolved measurements are not always possible in practice. The first method we introduce here is a convolution of the electric field with a sinc function in the frequency domain, which is equivalent to restricting the width of the signal in the time domain, and may in practice be approximated by other spectral filtering functions. First, we analyze the effect of reflected pulses on the imaging performance. To know when the reflections appear at the output, the time dependent electric field equivalent to Fig. 1(b) is obtained by applying the Fourier transform as shown in Fig. 2(a). The reflections supported by the WM arrive after 6.7 ps. In order to investigate the effect of the first reflected pulse, we apply a convolution with a sinc corresponding to a temporal gate width to 12 ps to the frequency resolved fields. Fig. 2(b) shows that the resulting intensity profile is similar to the profile obtained in Fig. 1(b), in that it has significant side lobes. However, the amplitude of these side lobes decreases, but their

spectral periodicity remain same, as expected. This indicates that even a single reflected pulse can severely deteriorate image quality.

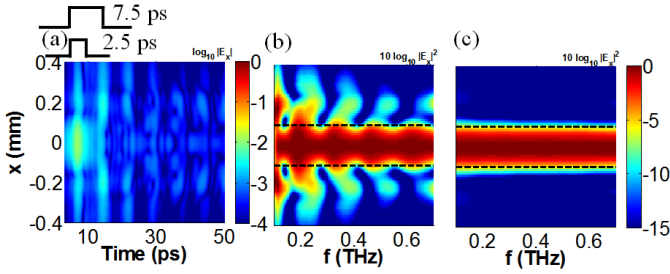


Fig. 2. (a) Simulated time dependent electric field after 1 mm WM. Simulated electric field intensity after convolution for different width of the gate function (b) 12 ps and (C) 8 ps.

Convoluting with a gate function of width 8 ps captures the main pulse only. The periodic side lobes are then completely eliminated over the frequency range considered significantly improving image quality. Other filter functions that can readily be implemented in experiments such as convolution with a rectangular function (i.e. spectral averaging) also provide considerable imaging improvements.

While we excite the aperture with an  $x$ -polarized plane wave, diffraction at the aperture generates  $y$  and  $z$  components and the field couples to both non-diffracting extraordinary waves and diffracting ordinary waves. The latter may add additional noise to the image, and the contribution of these waves depends on object size [8]. When the object size is smaller than the diffraction limit it cannot dominantly excite ordinary waves since their spatial frequencies do not overlap with those of propagating ordinary waves. However for objects larger than the wavelength, diffracting ordinary waves can become predominant and add considerable noise.

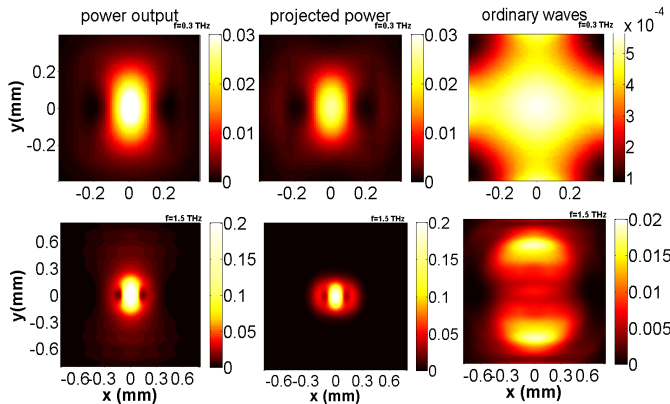


Fig. 3. Simulated 2D images of the single aperture at 0.3 THz (top row), and at 1.5 THz (bottom row).

This noise can be removed by filtering out the ordinary waves, imaging using the extraordinary waves only. As the polarization of extraordinary waves depends on wavevector, this requires projecting the field in the spatial Fourier domain, in which ordinary waves are orthogonal to both the wavevector and the wires, and the extraordinary waves are in the plane of the wires and the wavevector. Having measured both transverse components of  $\mathbf{E}$ , the extraordinary wave contribution,

$\mathbf{E}_e(\mathbf{k}_t)$  can be extracted in the Fourier domain by the following projection:

$$\mathbf{E}_e(\mathbf{k}_t) = \frac{\mathbf{E}(\mathbf{k}_t) \cdot \mathbf{k}_t}{|\mathbf{k}_t|^2} \mathbf{k}_t$$

where  $\mathbf{k}_t$  is the wavevector in the  $x, y$  plane. Finally, an image is obtained in direct space by taking the inverse Fourier transform of  $\mathbf{E}_e(\mathbf{k}_t)$ . Figure 3 summarizes the simulated results of power output, projected power, and contribution of ordinary waves for a single aperture. Since the incoming wave is  $x$ -polarized, ordinary waves will be excited predominantly in the  $y$  direction, resulting in spreading along  $y$ . Now we investigate the effect of ordinary waves for different sizes of apertures. For this, first we image a 200  $\mu\text{m}$  diameter aperture at 0.3 THz. At this frequency the aperture size is below diffraction limit. The projected power is shown in the middle column which is similar to the power output, meaning that the projection does not substantially improve the image quality. The reason is that the aperture size is below the diffraction limit, and does not excite ordinary waves as shown in the last column (note the scale). The ordinary wave is calculated by subtracting projected power from the power output. Now we calculate the image of a 300  $\mu\text{m}$  diameter aperture at higher frequency, 1.5 THz; the aperture is larger than the diffraction limit and can dominantly excite ordinary waves, as can be seen from the last column of bottom row. The projection here provides a remarkable improvement to the image quality.

In conclusion, we have seen that imaging from a WM based hyperlens suffers from severe artefacts that limit their use for broadband imaging. We introduced post-processing methods to eliminate the unwanted artefacts so that imaging can be performed over wide frequency bands. Additionally, diffracting ordinary waves can be removed by extracting only extraordinary waves using an appropriate projection, considerably improving image quality when imaging large objects.

## REFERENCES

- [1] A. Poddubny, I. Iorsh, P. Belov, and Y. Kivshar, "Hyperbolic metamaterials," *Nat. Photon.*, vol. 7, pp. 948-957, Nov. 2013.
- [2] A. Tuniz et al., "Imaging performance of finite uniaxial metamaterials with large anisotropy," *Opt. Lett.*, vol. 39, pp. 3286-3289, June 2014.
- [3] P. A. Belov, Y. Hao, and S. Sudhakaran, "Subwavelength microwave imaging using an array of parallel conducting wires as a lens," *Phys. Rev. B*, vol. 73, pp. 033108, Jan. 2006.
- [4] P. A. Belov, C. R. Simovski, and P. Ikonen, "Canalization of sub-wavelength images by electromagnetic crystals," *Phys. Rev. B*, vol. 71, pp. 193105, May 2005.
- [5] J. G. Hayashi, S. C. Fleming, B. T. Kuhlmeiy, and A. Argyros, "Metal selection for wire array metamaterials for infrared frequencies," *Opt. Express*, vol. 23, pp. 29867-29881, Nov. 2015.
- [6] A. Tuniz et al., "Drawn metamaterials with plasmonic response at terahertz frequencies," *App. Phys. Lett.*, vol. 96, pp. 191101, May 2010.
- [7] A. Tuniz et al., "Metamaterial fibres for subdiffraction imaging and focusing at terahertz frequencies over optically long distances," *Nat. Comm.*, vol. 4, pp. 2706, Oct. 2013.
- [8] A. Tuniz and B. T. Kuhlmeiy, "Two-dimensional imaging in hyperbolic media-the role of field components and ordinary waves," *Sci. Rep.*, vol. 5, pp. 17690, Dec. 2015.
- [9] K. J. Korbinian et al., "Ultra-broadband perfect imaging in THz wire media using single-cycle pulses," *Optica*, in press.